Available online at www.sciencedirect.com
SCIENCE DIRECT®
Journal of Solid State Chemistry 170 (2003) 450–457
JOURNAL OF SOLID STATE CHEMISTRY
http://elsevier.com/locate/jssc

Luminescent properties of the potassium zinc phosphates of composition $K_{1-x}Tl_xZn(PO_3)_3$

A. El Abiad,[a] M. Mesnaoui,[a] M. Maazaz,[a] C. Parent,[b,*] and G. Le Flem[b]

[a] *LCSM, Faculté des Sciences Semlalia, B.P.S 23 90, Marrakech, Maroc*
[b] *ICMCB, UPR CNRS 9048, 87, Av. du Dr Albert Schweitzer, 33608 Pessac Cedex, France*

Received 23 July 2002; received in revised form 6 November 2002; accepted 14 November 2002

Abstract

Crystalline and glassy $K_{1-x}Tl_xZn(PO_3)_3$ polyphosphates have been synthesized and characterized. UV–visible spectroscopy was systematically used in order to analyze the optical properties of Tl^+ ions both in crystalline and glassy forms with the similar compositions. The investigated polyphosphates can be considered as a model system since the spectroscopic properties of Tl^+ ions in the glasses could be deduced by comparison with those in crystals. From structural point of view, in the crystalline forms the thallium ions are six-fold coordinated in a dissymmetrical oxygenated sites. Three luminescences (α, A_X, A_T) have been then observed and were attributed to the isolated Tl^+ ions. In the glassy forms, an additional luminescence (D) has been detected in the low-energy range and was assigned to the Tl^+ pairs formation. The relationship between the Tl^+ site symmetry and its optical properties is discussed in the context of the Fukuda's model.

Keywords: Phosphates; Tl^+ luminescence; Glasses

1. Introduction

The luminescence of Tl^+ in insulators was first reported as Tl^+ was introduced as impurity in alkali halides. The emission and absorption spectra were interpreted by Seitz in the case of KCl:Tl assuming Tl^+ ions replaced K^+ in the lattice [1]. Later Curie [2] gave a basis of the interpretation of the spectroscopic properties of Tl^+ in alkali halides involving the "s^2" character of this ion. In several sodium chloride type compounds three absorption bands are usually observed labeled A, B, C with increasing energy in addition to a D band which has an excitonic character. In this simple description are excluded the additional bands resulting from possible clustering of this activator. Assuming Tl^+ in a cubic center the A, B, C bands were attributed, respectively, to the $^1A_{1g} \rightarrow {}^3T_{1u}$, $^3E_u + {}^3T_{2u}$ and $^1T_{1u}$ transitions, respectively. Actually, by excitation in the A bands, one or two emissions can be observed depending of the composition of the host. The origin of this effect was discussed in detail by Fukuda [3] and Ranfagni et al. [4]. The existence of two emission bands—A_T (high energy) and A_X (low energy)—was explained by considering the respective influence of spin–orbit coupling and electron–lattice interaction through the Jahn–Teller effect of the $^3T_{1u}$ excited state. Similar considerations were taken into account to explain the luminescent properties of the phosphor $Ca_3(PO_4)_2$:Tl used in fluorescent lamps [5]. The structure of β $Ca_3(PO_4)_2$ is characterized by five non-equivalent positions for Ca^{2+} with a wide range of coordination and calcium–oxygen distances which are included between 2.24 and 3.23 Å. Such multi-site system makes difficult the interpretation of the luminescent properties in relation to the crystal structure. Recently, similar A_X and A_T band emissions were observed for the phosphate $TlZn(PO_3)_3$ by varying both the excitation energy and the temperature and the whole properties were related to the stereo-activity of the Tl^+ $6s^2$ lone pair [6].

In oxide glasses a unique band emission is usually observed whatever the base glass composition and is generally assigned to the $^3P_1 \rightarrow {}^1S_0$ transition [7,8]. In the case of the Na_2O–P_2O_5 glass system, the excitation and emission bands undergo a red shift with increasing Na_2O concentration [9]. This effect, in accordance with

*Corresponding author. Fax: +33-5-56-84-27-61.
E-mail address: parent@icmcb.u-bordeaux.fr (C. Parent).

0022-4596/03/$ - see front matter © 2003 Elsevier Science (USA). All rights reserved.
doi:10.1016/S0022-4596(02)00165-2

the optical basicity concept, was explained in terms of change of the bonding between the Tl^+ ions and the oxygen atoms of the sites they occupy.

The present investigation examines the relationships between the crystal structure and the luminescent properties of the phases appearing in the system $K_{1-x}Tl_xZn(PO_3)_3$. The properties of glasses with same composition will be also described. The data will be discussed using a solid-state chemistry approach with the object of tentatively involving and reconciling all the previous results.

2. Experimental

The crystallized phosphates $K_{1-x}Tl_xZn(PO_3)_3$ ($0 \leqslant x \leqslant 1$) were prepared by heating pellets of stoechiometric mixtures of finely ground starting materials corresponding to the reaction:

$$x/2Tl_2CO_3 + ZnO + \frac{(1-x)}{2}K_2CO_3 + 3(NH_4)_2HPO_4 \rightarrow K_{1-x}Tl_xZn(PO_3)_3 + 6NH_3 + \frac{1}{2}CO_2 + \frac{9}{2}H_2O.$$

The mixtures were heated during 15 h at 200°C and 250°C. For the rich potassium compounds, the reagents were continuously heated at 320°C for 24 h. In this range of compositions ($x \leqslant 0.2$) there exist two allotropic forms. The high temperature form is obtained through a heat treatment at 550°C followed by a quenching of the samples at room temperature. The final thermal treatment of the rich thallium compounds is carried out at 500°C for 12 h. All the samples are white.

Glasses were made by melting mixtures of $K_{1-x}Tl_xZn(PO_3)_3$ compositions at 900°C for 4 h. The melts were poured onto a brass block heated at 280°C and annealed at this temperature for 15 h. The glass transition temperatures decrease from 352°C ($x = 0$) to 296°C ($x = 1$). The samples used for spectroscopic investigation were carefully polished to produce disks of 1 mm thickness with parallel faces. The evolution of the density as a function of the thallium concentration are given in Table 1. The densities were obtained by immersing the samples in calibrated diethyl orthophtalate.

The crystalline samples were checked by X-ray diffraction analysis. Absorption spectra were obtained using a Shimadzu UV-301 spectrophotometer and excitation/emission spectra using a Spex FL212 spectrofluorophotometer. The IR spectra were recorded using a Nicolet 6X spectrometer in the 400–1400 cm^{-1} region.

Table 1
Variation of the densities vs thallium concentration

X	0	0.3	0.6	0.8	1.00
Density ± 0.03	2.68	2.94	3.40	3.72	3.91
Thallium concentration 10^{21} ions/cm^3	0	1.22	2.79	3.78	4.64

3. Structure of the crystalline phases appearing in the $K_{1-x}Tl_xZn(PO_3)_3$ system

The structures of the involved phases of the $K_{1-x}Tl_xZn(PO_3)_3$ system were previously described [6,10]. Two allotropic forms are found in the range of composition $0 \leqslant x \leqslant 0.2$. For $0.6 \leqslant x \leqslant 1$ the phase belongs to the $TlZn(PO_3)_3$ structure type. In the intermediate range of composition is observed a mixture of the limiting phases corresponding to $x = 0.2$ and 0.6.

The structure of the low temperature form (LTF) of $KZn(PO_3)_3$ is characterized by long phosphate chains running along the $\vec{c}$ direction whereas in the high temperature form (HTF) the basic phosphorus oxygen structure unit is a $[P_3O_9]$ ring anions consisting of three $[PO_4]$ tetrahedra sharing two corners with the two others. In the two phosphate frameworks the zinc and the potassium are located, respectively, in octahedral and anti-prismatic sites. For the low temperature form the anti-prismatic and octahedral sites share faces, giving rise to infinite chains along the $\vec{c}$ direction with a 1–1 potassium zinc ordering. The cationic ordering of the high temperature form can be described by (a, b) planes of edge-sharing $[ZnO_6]$ octahedra and $[KO_6]$ antiprisms (Fig. 1). The relevant shortest inter-atomic distances are given in Table 2. Assuming a substitution of thallium for potassium as x increases, the Tl^+ ions can be considered as isolated in both phases.

The structure of the rich thallium solid solution have been studied for the compound $TlZn(PO_3)_3$ [10]. In this polyphosphate the Tl^+ ions are located in tunnels created by the Zinc polyphosphate network $[Zn(PO_3)_3]$. The thallium atoms are found in a unique crystallographic site with a disymmetric configuration and the coordination number by oxygens determined by bond calculation is 6 (Fig. 2). The three Tl–O distances are

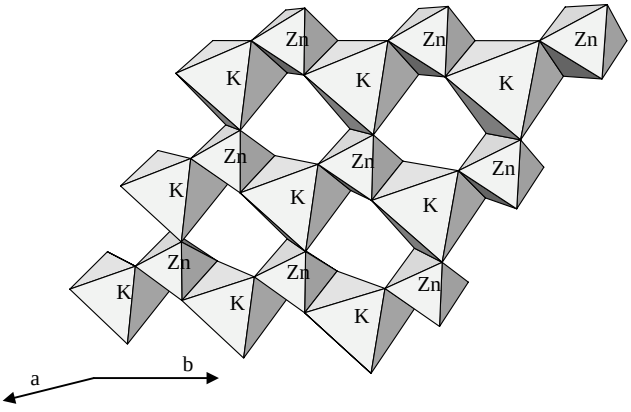

Fig. 1. Connection between the $[ZnO_6]$ and $[KO_6]$ polyhedra in HTF–$KZn(PO_3)_3$.

included between 2.736 and 3.278 Å. Such large distances induce a low stereo-chemical activity of the $6s^2$ lone pair. The effect of the stereoactivity of the $6s^2$ lone pair leads to the formation of [Zn,TlO_6] corrugated chains along the $\vec{a}$ axis. The shortest Tl–Tl distance is 5.14 Å. Therefore, the Tl^+ as luminescent center can be considered as isolated from each other.

4. Structural investigation of the glasses by infrared spectroscopy

The absorption threshold of the glass of composition $KZn(PO_3)_3$ was found at 220 nm which is typical of oxygen–phosphorus charge transfer [11].

The infrared spectra of powder samples of the both forms of $KZn(PO_3)_3$ have been compared with the spectra of glasses of composition $x = 0$, 0.5 and 1. The assignments of all observed bands are given in Table 3, in agreement with the data of Rulmont et al. [12] and Martin [13]. According to these authors, whatever the "chain" or "ring" arrangement of [PO_4] groups in polyphosphates, strong IR bands are found around 1300–1250 cm^{-1} (ν_{as} PO_2) and around 1200–1050 cm^{-1} (ν_s PO_2). Moreover, the chain structures are typically characterized by a broad band around 900 cm^{-1} whereas small rings exhibit specifically a very narrow band of strong intensity between 780 and 765 cm^{-1}. Here the ν_s P–O–P vibration is found at 775 cm^{-1} for the HTF $KZn(PO_3)_3$ which contains the small P_3O_9 rings. Thus exists a good agreement between the structures of the crystalline phases and their IR spectra. Accordingly the observed bands of the glass compounds are typical of the association of the [PO_4] groups with chain structures.

Table 2
Relevant inter-atomic distances for the two forms of $KZn(PO_3)_3$ [6,10]

Distances(Å)	LTF–$KZn(PO_3)_3$	HTF–$KZn(PO_3)_3$
Zn–O	2.043×6	$\approx 2.120 \times 6$
K–O	2.855×6	$\approx 2.750 \times 6$
n-nK–Zn*	3.483×2	$\approx 3.813 \times 3$
n-n K–K*	6.303×2	$\approx 4.886 \times 2$

n-n stands for nearest neighbors.

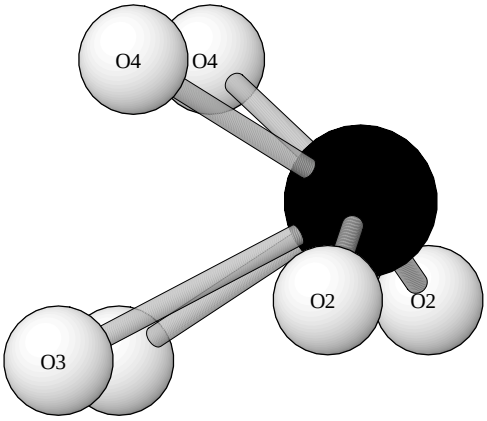

Fig. 2. Thallium environment in the structure of $TlZn(PO_3)_3$.

5. Luminescent properties

5.1. Crystalline phases

Similar luminescent properties were observed for the two phases of the $0 < x \leqslant 0.2$ composition range. The phosphates exhibit three emissions with maxima observed, respectively, at 270 nm (α), 330 nm (A_T) and 395 nm (A_X, LTF) or 410 nm (A_X HTF) (Fig. 3). As the excitation wavelength increases from 230 to 260 nm, the intensity of α decreases whereas the intensities of A_T and A_X increase. The excitation band of α exhibits a maximum at 230 nm. The excitation bands of A_T and A_X exhibit, respectively, a maximum at 240 and 250 nm. The overlapping between the (α) emission and the excitation band of A_T and A_X allows an efficient energy transfer from α to A_T and A_X (Fig. 4). An increasing Tl concentration tends to decrease weakly the α emission intensity (Fig. 5).

The luminescent properties of the rich thallium phase ($x \geqslant 0.6$) were studied in detail for the $TlZn(PO_3)_3$ composition. The emission and excitation spectra have been investigated between 6 and 300 K.

Under a 250 nm excitation, the emission spectrum recorded at 6 K exhibits a broad band which can be decomposed into two components peaking, respectively, at 325 nm (A_T) and 380 nm (A_X) (Fig. 6). The excitation spectrum of the A_X emission is a broad band peaking at

Table 3
Infra-red bands of the phosphate of composition $K_{1-x}Tl_xZn(PO_3)_3$

Compounds assignments (cm^{-1})	LTF $KZn(PO_3)_3$	HTF $KZn(PO_3)_3$	Glass $x = 0$	Glass $x = 0.5$	Glass $x = 1$
ν_{as} PO_2	1250	1290	1265	1264	1262
ν_s PO_2	1150, 1170	1120, 1050	1087	1120	1120
ν_{as} $(P–O–P)_{cycl}$		940			
$\nu_{as}(P–O–P)_{chain}$	870		900	902	896
ν_s $(P–O–P)_{cycl}$		775, 645			
ν_s $(P–O–P)_{chain}$	745, 675		742	760	766, 750

cycl. and chain labeled, respectively, the ring and chain arrangement of the PO_4 groups.

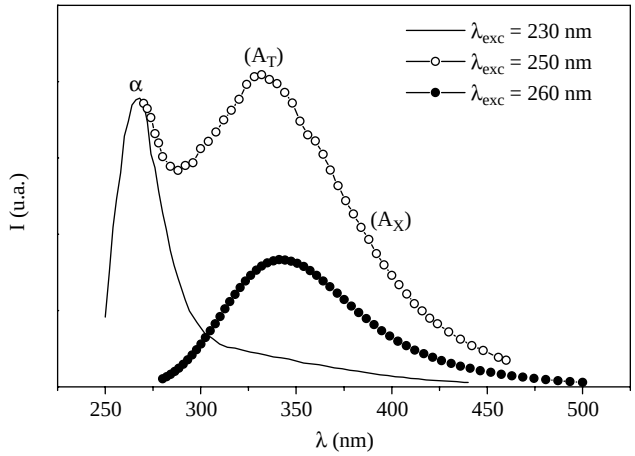

Fig. 3. Evolution of emission bands (α), (A_X) and (A_X) as a function of excitation wavelength for $K_{0.95}Tl_{0.05}Zn(PO_3)_3$ (HTF) at $T = 300$ K.

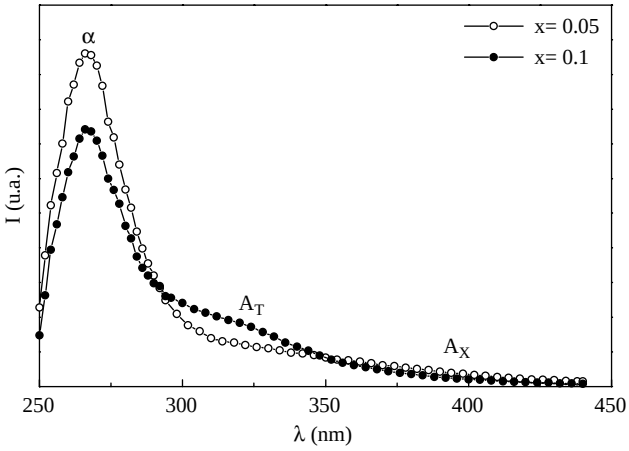

Fig. 5. Emission spectra for the crystalline HTF–$K_{1-x}Tl_xZn(PO_3)_3$ under a 230 nm excitation.

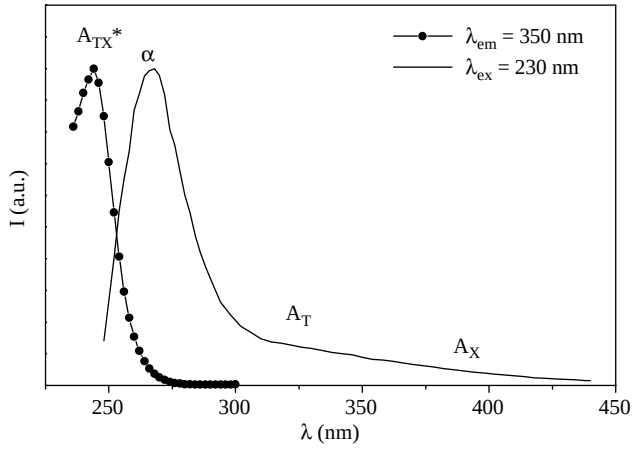

Fig. 4. Overlapping between the (α) emission and the (A_T) and (A_X) excitation for $K_{0.95}Tl_{0.05}Zn(PO_3)_3$ (HTF).

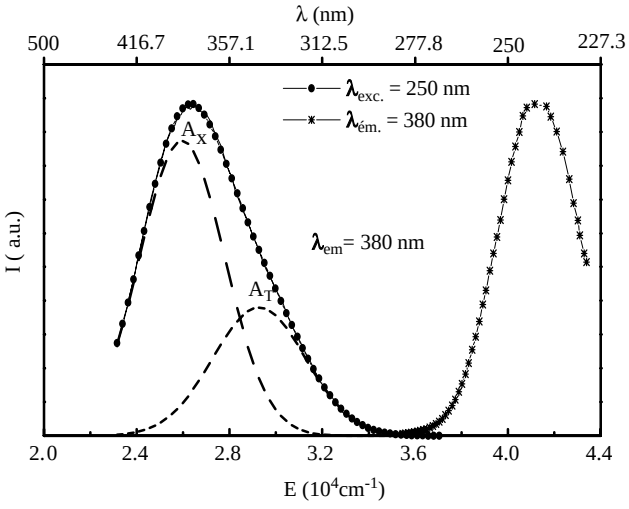

Fig. 6. Excitation ($\lambda_{em} = 380$ nm) and emission ($\lambda_{exc} = 250$ nm) spectra of $TlZn(PO_3)_3$ at $T = 6$ K.

243 nm whereas the excitation spectrum of the A_T emission can be localized at about 230 nm (this range of energy corresponds to the experimental limit of the fluorescence detection). An additional band with low intensity can be detected at 250 nm (Fig. 7). By increasing the temperature the A_T emission intensity decreases whereas the A_X emission intensity increases. Only this last emission is observed at room temperature. At room temperature the A_T emission increases with increasing thallium concentration.

Under a 230 nm excitation only the A_T emission is observed whatever the temperature with a slight blue shift of the band maximum (Fig. 8).

5.2. Glasses

In the glasses the progressive introduction of thallium red shifted the absorption threshold by the appearance of a strong band due to the $^1S_0 \rightarrow {}^3P_1$ transition.

As an example Fig. 9 exhibits the emission spectrum of the glasses of composition $K_{0.95}Tl_{0.05}Zn(PO_3)_3$ under a 230 nm excitation at $T = 300$ K. A broad band covering the UV–visible region is observed which can be decomposed into three bands peaking, respectively, at 280 nm (α), 310 nm (A_T) and 360 nm (A_X). By increasing the excitation wavelength (230→250 nm) the (α) emission intensity decreases whereas the intensities of A_T and A_X increase. The effect of increasing the thallium concentration or wavelength excitation leads to decrease the (α) intensity emission and to increase both A_T and A_X emissions. Simultaneously appears a new large band peaking at 430 nm labeled D which reaches its maximum for $x = 1$ and $\lambda_{exc} = 370$ nm (Fig. 10). The maxima of the excitation band for these emissions are observed, respectively, at 235 nm (α), 250 nm (A_T and A_X) and 370 nm (D). In the excitation spectrum of D is also observed a broad maximum covering the

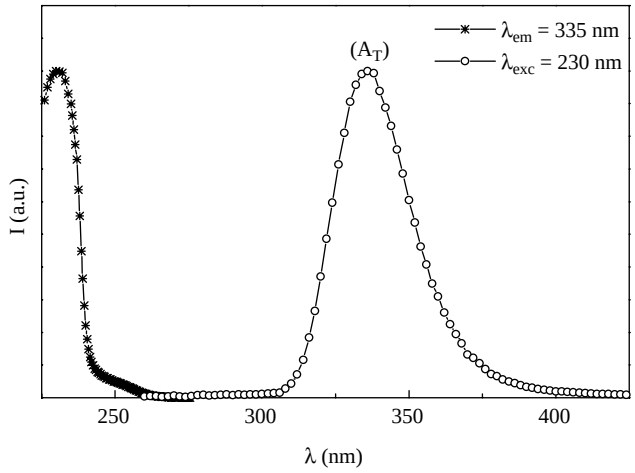

Fig. 7. Excitation ($\lambda_{em} = 335$ nm) and emission ($\lambda_{exc} = 230$ nm) spectra of $TlZn(PO_3)_3$ at $T = 6$ K.

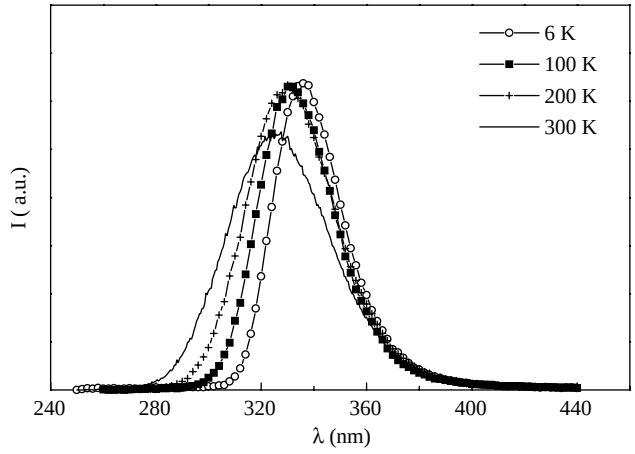

Fig. 8. Thermal variation of the A_T emission of $TlZn(PO_3)_3$ under a 230 nm excitation.

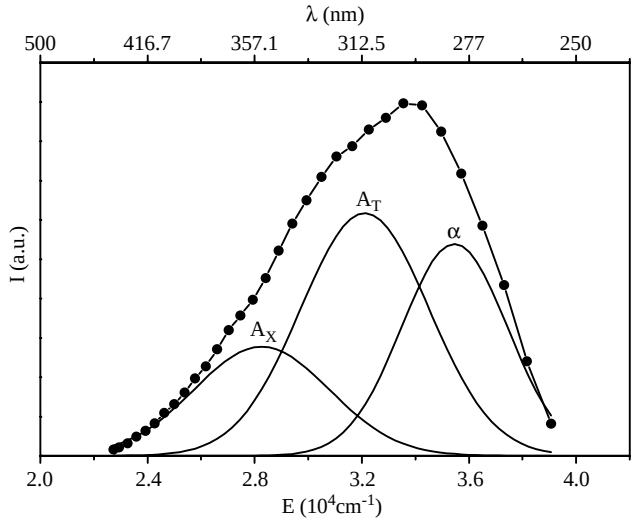

Fig. 9. Emission spectra recorded under a 230 nm excitation for the $K_{0.95}Tl_{0.05}Zn(PO_3)_3$ glass at 300 K.

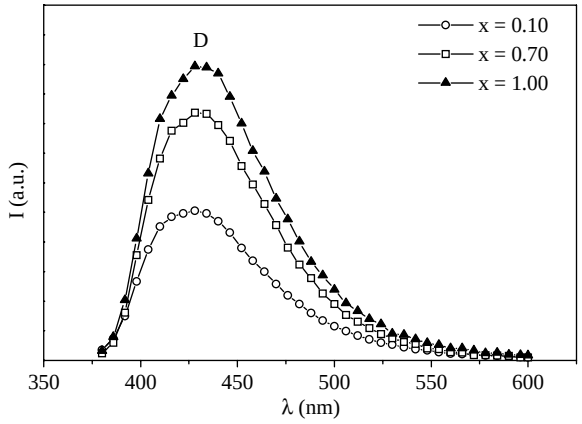

Fig. 10. Emission spectra recorded under a 370 nm excitation for the$K_{1-x}Tl_xZn(PO_3)_3$ ($0 < x \leqslant 1$) glasses at 300 K.

230–250 nm region which is the signature of $(A_T) \rightarrow (D)$ energy transfer.

6. Discussion

6.1. Structural properties

The structural evolution observed in the phases of the $K_{1-x}Tl_xZn(PO_3)_3$ system must be discussed with respect to the thallium environment. For the crystalline phases related to the low and high temperature forms of $KZn(PO_3)_3$, the Tl is assumed to be located in the potassium site i.e., in the corresponding antiprismatic (K–O = 2.85 Å) and distorted octahedral (K–O = 2.75 Å) sites. As previously mentioned the K(Tl) ions can be considered as isolated from each other in both structure types as a result of the cationic distribution. Therefore, the luminescence can be attributed to isolated Tl^+ center in distorted octahedral coordination.

In the structure of $TlZn(PO_3)_3$ the thallium are also isolated from each other. On the other hand, they are located in strongly irregular site, typical of lone pair ions, in a wide cavity limited by 15 oxygens. Bond valence calculations are in agreement with a reduced coordination polyhedron defined by the six oxygen atoms of the two ZnO_6 nearest-neighbor octahedra but with Tl–O distances ranging from 2.736 to 3.278 Å. Apparently, such structural features make the Tl^+ luminescent center different from the previous ones.

A tentative investigation of the Tl environment in glasses by X-ray absorption spectroscopy failed and the luminescent properties will be discussed by comparison with that of the crystalline phases.

6.2. Luminescent properties

6.2.1. Theoretical introduction

The Tl^+ luminescence involves $6s^2 \leftrightarrow 6s6p$ transitions. The $6s^2$ electronic configuration is responsible for the

Table 4
Comparison between the luminescent properties of Tl-doped potassium halogenides and of the investigated crystallized phosphates

Compound λ_{em} ($T = 300$ K)	$\alpha\ ^1P_1$	$A_T\ ^3P_1$	$A_X\ ^3P_1$	Ref.
KF:Tl	224 exc. in (C)	289 exc. in (A)		[2,3] and references herein
KCl:Tl	247 exc. in (C)	297 exc. in (A)	297 exc. in (A)	[2,3] and references herein
KBr:Tl		308 exc. in (A)	354 exc. in (A)	[2,3] and references herein
KI:Tl	272 exc. in (C)	335 exc. in (A)	429 exc. in (A)	[2,3] and references herein
$\beta Ca_3(PO_4)_2$:Tl^+		310 λ_{exc} 243	336 λ_{exc}. 243	[5]
$KZn(PO_3)_3$:Tl LTF phosphate chains K–O = 2.85 Å K–Zn = 3.82 Å × 2	270 λ_{exc} 230	340 λ_{exc} 260	395 λ_{exc}. 260	This work
$KZn(PO_3)_3$:Tl HTF phosphate cycles K–O ≈ 2,75 Å K–Zn = 3.48 Å × 3	270 λ_{exc}. 230	340 λ_{exc}. 260	410 λ_{exc}. 260	[6]
$TlZn(PO_3)_3$ phosphate chains 2.73 < Tl–O < 3.27 Å		335 λ_{exc}. 250	380 observed only at low temperatures λ_{exc}. 250	

Only isolated emitting centers are considered.

$^1S_0$ ground state whereas the first $6s6p$ excited states are successively $^3P_0$, $^3P_1$, $^3P_2$ and $^1P_1$ with increasing energy. Tl^+ luminescence was first investigated in Tl-doped alkali halides which can be considered as model systems [2]. The main problem results from the existence of a double luminescence emission which can be observed as some of these phosphors are excited in the (A) [$^1A_{1g} \rightarrow {}^3T_{1u}$] absorption band. Actually, it was admitted that Jahn–Teller effect (JTE) causes the splitting of the T states and corresponding adiabatic potential energy surfaces (APES) can be calculated by varying the parameters governing the system, mainly the spin–orbit interaction as compared with the electron–phonon interaction (JTE). Such calculations were first carried out in the framework of the Russel–Saunders coupling followed by a more general approach involving intermediate coupling [2,4]. Within this context two kinds of minimum—related to the appearance of tetragonal or rhombic distortion—were predicted. They can coexist in a wide range of parameter values and are considered at the origin of the double luminescence. The following discussion will take into account such theoretical background which allows the attribution of the excitation and emission bands.

6.2.2. *Crystallized phosphates*

Table 4 compares the location of the emission bands of the Tl-doped potassium halides and of the industrial phosphor $\beta Ca_3(PO_4)_2$–Tl with those of the investigated crystalline phosphates.

The high-energy emission observed for $x \leqslant 0.2$ corresponds to the $^1P_1 \rightarrow {}^1S_0$ transition on the Tl^+. The two lower energy emissions can be considered as originating from the two minima on the adiabatic potential energy surface (APES) of the ^3P excited state relaxed by the Jahn–Teller effect. In the potassium halides, the red shift of the emission bands when going from one ligand environment to the other in the sequence of F^-, Cl^-, Br^-, I^- ligands is typical of the nephelauxetic effect. It corresponds to a correlative decrease of the sp frequency. In contrast, due to the strong covalent character of the P–O bond, the Tl–O bond can be considered as ionic in agreement with the rather large Tl–O distance observed for instance in $TlZn(PO_3)_3$. For comparison the two Tl–O distances found in Tl_2O are, respectively, 2.52 and 2.54 Å [14]. The phosphates structures are less closely packed than that of the potassium halides and this decreasing stiffness will result in an increase of the Stokes shift. As previously mentioned for the compounds with $x \leqslant 0.2$ the Tl^+ sites can be considered as distorted octahedra i.e., almost identical with the site of sodium chloride type compounds which is not true for $TlZn(PO_3)_3$ where the Thallium environment involves oxygens with a large distribution of the Tl–O distances.

In Tl-doped potassium halides and related compounds, the A_T emission is first observed at low temperature with a small percentage of the A_X emission. As the temperature increases, the A_T emission decreases whereas the A_X emission increases in proportion depending on the considered compounds. In the phosphates with low thallium content ($x \leqslant 0.2$) both emissions are observed at room temperature. In the case of $TlZn(PO_3)_3$ which has been investigated in detail the thermal evolution of the A_T and A_X emission intensities are exactly opposite to the behavior observed in potassium halides. The low value of the thermal quenching temperature for A_X is the signature of a large Stokes shift. In these conditions, hypothetical configuration curves for the $^1S_0$, $^3P_1$ and $^1P_1$ levels can account for the experimental data (Fig. 11). At low temperature, a 250 nm excitation populates preferentially X and also T minima whereas a 235 nm excitation populates only T trough the G crossing point connecting the $^1P_1$ and the $^3P_1$ curves. In the former case as the temperature is raised, T is populated at the expense of X. In the second case only T is populated whatever the temperature.

Finally, the concentration quenching of the (α) emission can be explained by two mechanisms: either a

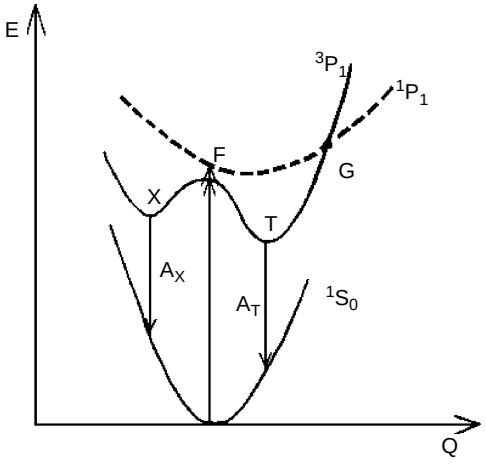

Fig. 11. Hypothetical configuration curves of the thallium $^1S_0$, $^3P_1$, and $^1P_1$ levels. The T and X minima stand for the respective origins of the A_T and A_X emissions.

Table 5
Luminescent properties of the $K_{1-x}Tl_xZn(PO_3)_3$ glasses for the isolated emitting center

Glass composition $K_{1-x}Tl_xZn(PO_3)_3$	α $^1P_1$	A_T $^3P_1$	A_X $^3P_1$
$X = 0.05$, $\lambda_{exc} = 230$ nm	277	312	357
$X = 0.5$, $\lambda_{exc} = 230$ m		312	357
$X = 1$, $\lambda_{exc} = 230$ nm		312	367

Table 6
Spectral data for the Tl-doped Na_2O–P_2O_5 glass system according to Duffy et al. (9)

Na_2O–P_2O_5 glasses [9]	λ_{em} (nm)	λ_{exc} (nm)	Stokes shift (cm^{-1})
20% Na_2O	283	225	9200
30% Na_2O	283	224	9400
40% Na_2O	284	225	9300
50% Na_2O	298	226	10,800
62% Na_2O	349	230	14,800

shift of the $^1P_1$ configuration curve allowing the crossing G point (Fig. 11) to be at energy below that of the F point or an energy transfer between two Tl^+ ions which can be deduced by the overlapping between the (α) emission band and the A_X, A_T excitation bands (Fig. 7). This later mechanism would lead to a non-radiative filling of $^3P_1$ level at the expense of the $^1P_1$ level according to the scheme $^1P_1 \rightarrow {}^1S_0/{}^1S_0 \rightarrow {}^3P_1$.

6.2.3. *Glassy phosphates*

Table 5 summarizes the luminescent properties of the glasses as a function of the thallium concentration at 300 K. The high-energy excitation and emission ($\lambda_{exc} \approx 230$ nm, $\lambda_{em} \approx 270$ nm) correspond to the transition $^1S_0 \leftrightarrow {}^1P_1$ and the excitation and emission at lower energy ($\lambda_{exc} \approx 250$ nm, $\lambda_{em} \approx 310$ and 360 nm) results from the $^1S_0 \leftrightarrow {}^3P_1$ transitions, the A_X and A_T emissions being related to the Jahn–Teller relaxation. Such assignments are in complete agreement with the data of the crystalline phosphates. No significant variation of spectroscopic properties is detected as the thallium concentration increases since the former glass network is typical of phosphate chains in all range of compositions. The unique difference between the luminescent properties of the crystals and of the glasses is the appearance of low-energy emission and excitation bands ($\lambda_{exc} \approx 350$ nm; $\lambda_{em} \approx 470$ nm) associated with the formation of Tl^+ pairs. Such associations are excluded in crystals due to the 1–1 Tl^+–Zn^{2+} ordering induced by the size difference between these two ions.

In a previous paper Duffy et al. [9] apply the ultraviolet fluorescence spectroscopy to investigate the glass basicity using Tl^+ and Pb^{2+} as probe ions. In the spectral data collected for the Na_2O–P_2O_5 glass system, the measured energy excitation of the Thallium luminescence was found approximately constant between 44,500 and 43,400 cm^{-1} ($\lambda = 225-230$ nm) (Table 6). According to the result of this investigation the attribution of this excitation to the $^1S_0 \rightarrow {}^3P_1$ transition seems questionable as well as the interpretation of the emission spectra. Actually, in these systems the energy difference between the $^1P_1$ and $^3P_1$ levels is small. On the other hand, the luminescent centers are distributed in multi-sites. Both factors make difficult the interpretation of the data and in this context the comparison with the properties of crystalline materials can be useful.

In conclusion the luminescent properties of the thallium zinc phosphates—crystals or glasses—are quite similar and can be described in the context of the model proposed for the Tl-doped alkali halides. The large Tl–O distances observed in the phosphates weakens the effect of the crystal field which is also in agreement with the weak chemical effect of the $6s^2$ lone pairs.

7. Conclusion

The crystallographic and optical investigations contribute to clarify significantly the Tl^+ photoluminescence in phosphate materials—crystalline and glassy forms—which was still an unexplored area. The relationship between the local environment of Thallium ion and its luminescence properties is established on the basis of the Fukuda's theory. Basically, Tl^+ ion, when isolated in its six-fold oxygenated site, gives rise to three ultra-violet luminescences (α, A_X, A_T) both in crystalline and glassy phosphates. (α) Emission is attributed to $^1P_1 \rightarrow {}^1S_0$ electronic transitions while (A_X) and (A_T) bands are ascribed to $^3P_1 \rightarrow {}^1S_0$ transitions according to a partial splitting of $^3P_1$ emitting level enhanced by Jahn–Teller effect. The (D) visible luminescence,

detected uniquely in glassy forms, is assigned to Tl^+ pairs formation. The presence of such thallium—pair emission in the glassy form of the investigated phosphates suggests that the thallium—zinc ordering observed in the crystals is not entirely preserved in glasses.

References

[1] F. Seitz, J. Chem. Phys. 6 (1938) 150.
[2] D. Curie, in: Gauthier-Villars (Ed.), Champ Cristallin et Luminescence, Paris, 1968, p. 162.
[3] A. Fukuda, Phys. Rev. B 1 (10) (1970) 4161.
[4] A. Ranfagni, G. Viliani, J. Phys. Chem. Solids 35 (1974) 25.
[5] A.C. Van Der Steen, Th.J.A. Aalders, Phys. Stat. Sol. B 103 (1981) 803.
[6] A. El Abiad, B. Es-Sakhi, M. Mesnaoui, M. Maazaz, I. Belharouak, P. Gravereau, C. Parent, G. Wallez, G. Le Flem, J. Solid State Chem. 154 (2000) 584.
[7] A. Ghosh, J. Chem. Phys. 44 (2) (1966) 535.
[8] S. Parke, R.S. Webb, J. Phys. Chem. Solids 34 (1973) 85.
[9] J.A. Duffy, G.O. Kyd, Phys. Chem. Glasses 36 (3) (1995) 101.
[10] M.T. Averbuch-Pouchot, Bull. Soc. Mineral. Cristallogr. 95 (1972) 558.
[11] E. Nakazawa, F. Shiga, J. Luminescence 15 (1977) 255.
[12] A. Rulmont, R. Cahay, M. Liegeois-Duyckaerts, P. Tarte, Eur. J. Solid State Inorg. Chem. 28 (1991) 207.
[13] S.W. Martin, Eur. J. Solid State Inorg. Chem. 28 (1991) 163.
[14] H. Sabrowsky, Z. Anorg. Allg. Chem. 381 (1971) 266.